Monolithically Integrated InAsSb-Based nBnBn Heterostructure on GaAs for Infrared Detection

Chengzhi Xie, Vincenzo Pusino, Ata Khalid, Adam P. Craig, Andrew Marshall, and David R. S. Cumming

***Abstract*—The high-operating temperature infrared photodetectors with multicolor function that are capable of monolithic integration are of increasing importance in developing the next generation of the mid-IR image sensors. Applications of these sensors include defense, medical diagnosis, environmental, and astronomical observations. We have investigated a novel InAsSb-based nBnBn heterostructure that combines a state-of-the-art InAsSb nBn detector with an InAsSb/GaSb heterojunction detector. At room temperature, the reduction in the dark current density of more than an order of magnitude was achieved compared to the previously investigated InAsSb/GaSb heterojunction detectors. Electrical characterization from cryogenic temperatures to room temperature confirmed that the nBnBn device was diffusion limited for the temperatures above 150 K. Optical measurements demonstrated that the nBnBn detector was sensitive in both the SWIR and MWIR wavelength range at room temperature. The specific detectivity ($D*$) of the competed nBnBn devices was calculated to be 8.6×10^8 cm $\cdot$ Hz$^{1/2}$W^{-1} at 300 K and approximately 1.0×10^{10} cm$\cdot$Hz$^{1/2}$W^{-1} when cooled down to 200 K (with 0.3 V reverse bias and 1550-nm illumination). In addition, all the photodetector layers were grown monolithically on GaAs active layers using the interfacial misfit array growth mode. Our results, therefore, pave the way for the development of new active pixel designs for the monolithically integrated mid-IR imaging arrays.**

***Index Terms*—InAsSb, GaSb, high operating temperature, dual-color, infrared photodetector, monolithic integration, imaging arrays.**

I. Introduction

PHOTODETECTORS with multi-color function, capable of near room temperature operation are highly in demand for delivering the next generation of mid-infrared (mid-IR) imaging sensors [1]. Apart from the well-known applications in military, defense and security, these novel detectors will create opportunities in a number of civilian applications such as gas detection and biomedical diagnosis by significantly reducing the cost and size of the imaging systems [2], [3]. Mid-IR photodetectors based on HgCdTe (also known as MCT) have shown unbeaten detection performance owing to the long minority carrier lifetime [4]–[6]. However, the quality and reproducibility of growth of MCT materials is difficult to control. The resulting high-cost of MCT imagers has limited the widespread diffusion of this material for low-cost, large-volume applications [7]. Furthermore, there is requirement to find alternatives because new regulations on the use of Hg in industry are being introduced in Europe [8]. The quality of growth of Sb-based III-V semiconductors is much more consistent, and their manufacturing technology is also well-established. Among them, bulk InAsSb alloy has attracted considerable attention in recent years [9]. Its widely tunable bandgap and capability of lattice-matched growth on GaSb or AlSb buffers offers great flexibility for innovative designs such as the nBn photodetector. In a typical nBn design, a barrier (B) layer made by wide bandgap material is inserted between two n-type doped InAsSb layers (n) to block the flow of majority carriers through a large ($>$1 eV) conduction band offset. The resulting nBn structure can thus greatly suppress the dark currents generated from the InAsSb absorption layer, leading to near background limited performance (BLIP) at high operating temperature ($\sim$200 K) [10]–[12]. As a consequence, the devices need only thermoelectric cooling.

Recently, a novel growth technique called interfacial misfit array (IMF) growth mode was developed that allows buffer-free growth of high quality GaSb layers onto lattice-mismatched GaAs substrates [13], [14]. Growth of InAsSb nBn photodetector layers was also demonstrated on GaAs substrates using a high quality GaSb buffer layer prepared by the IMF technique [15]. The nBn detectors grown on GaAs substrate were reported to achieve comparable performance to the devices grown on more expensive GaSb substrates [16], [17]. These nBn photodetectors were tested with both top and bottom contacts made on two n-type doped InAsSb contact layers. To date, there has been no study of the performance of InAsSb nBn photodetectors with the bottom metal contact made on the n-type doped GaAs layer. On the other hand, previous studies showed that a n-type InAsSb/GaSb heterojunction demonstrated dual-color capability for detection of light at both short and medium infrared wavelengths (SWIR and MWIR) [18]–[20]. However, since photoconduction in the InAsSb/GaSb heterojunction detectors is associated with majority carriers, high dark current (mA order) and hence large shot noise is expected es-

Manuscript received February 1, 2018; revised March 27, 2018 and April 10, 2018; accepted April 12, 2018. Date of publication April 24, 2018; date of current version May 8, 2018. This work was supported by EPSRC under Grant EP/J018678/1 and EP/M01326X/1. (*Corresponding author: Chengzhi Xie.*)

C. Xie, V. Pusino, and D. R. S. Cumming are with the Electronics and Nanoscale Division, School of Engineering, University of Glasgow, Glasgow G12 8LT, U.K. (e-mail: chengzhi.xie@glasgow.ac.uk; vincenzo.pusino@glasgow.ac.uk; david.cumming.2@glasgow.ac.uk).

A. Khalid with the Centre of Electronic Warfare, Information and Cyber, Cranfield University, Defence Academy of the United Kingdom, Shrivenham SN6 8LA, U.K. (e-mail: Ata.khalid@cranfield.ac.uk).

A. P. Craig and A. Marshall are with the Department of Physics, Lancaster University, Lancaster LA1 4YB, U.K. (e-mail: a.craig1@lancaster.ac.uk; a.r.marshall@lancaster.ac.uk).

Color versions of one or more of the figures in this paper are available online at http://ieeexplore.ieee.org.

Digital Object Identifier 10.1109/JSTQE.2018.2828101

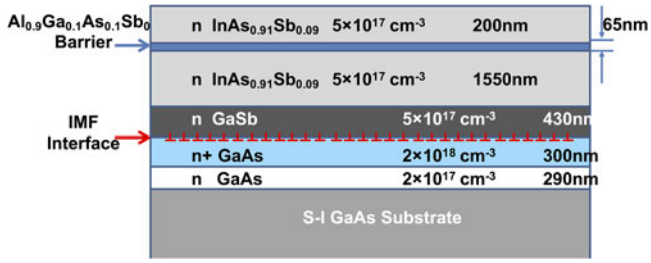

Fig. 1. Diagram of the material layer structure with the InAsSb nBn photodetector grown on to GaAs active layers using the IMF technique.

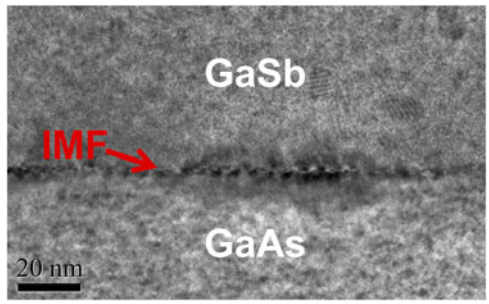

Fig. 2. Transmission electron microscopy (TEM) image of the IMF GaSb/GaAs interface, clearly showing the array of misfit dislocations between the GaAs layer (lower) and the GaSb layer (upper).

pecially when the detectors are biased for operation at room temperature.

In this paper, we report a novel infrared photodetector structure that combines a state-of-art InAsSb nBn structure with an InAsSb/GaSb/GaAs heterojunction diode. Since there is also a large band offset in the conduction band at the interface between InAsSb and GaSb [20], we refer to this new design as an nBnBn heterostructure for short. Section II of this paper describes the layer structure of the wafer and the device fabrication processes. Section III presents the DC characterization results of the completed nBnBn devices at both room temperature and cryogenic temperature. The detection performance of the devices was also measured in response to IR illumination. Finally, a summary of the work is presented in Section IV.

II. Experiment

The epitaxial layer structure used in this work is shown in Fig. 1. The material was grown on a 2-inch semi-insulating (SI) GaAs substrate, using a VG V80-H MBE reactor for growth of all layers. The wafer was first kept at 600 °C for ∼5 minutes to achieve oxide desorption from the GaAs substrate, then the temperature was reduced to 570 °C for growth of the GaAs active layers. The GaAs active layers consisted of a Si doped channel layer followed by a heavily doped contact layer. The GaAs active layers were added for the ultimate goal of implementing a MEtal Semiconductor Field Effect Transistor (MESFET), so that an active switching imaging array can be realized accordingly [21]–[23].

The IMF growth was then initiated by switching to a Ga terminated surface (through a cessation of As_2 overpressure for ∼5 sec) and then reducing the growth temperature to 510 °C under Sb_2 flux. Afterwards, the Ga shutter was opened, commencing GaSb growth. After initially exhibiting a spotty pattern (indicating 3D growth) the reflection high energy electron diffraction (RHEED) pattern changed to a streaked reconstruction after 10–20 monolayers (ML), indicating a good quality crystal layer. As illustrated in Fig. 2, the upwardly propagating threading dislocation density after the IMF growth is minimised. A dislocation density of around 10^8 cm^{-2} was obtained. Based on the work of others [13] we believe there is scope to improve this by a factor of 100 after optimization of growth conditions. Once the lattice has been transitioned to the lattice constant of GaSb (6.09 Å) in this way, InAsSb layers can be grown, so that they are effectively lattice matched to a thin "virtual substrate". Finally, a lattice matched InAsSb nBn photodetector was grown, including a non-intentionally doped $Al_{0.1}Ga_{0.9}As_{0.1}Sb_{0.9}$ barrier layer (AlGaAsSb in the following) sandwiched between a thick absorption layer and a thinner contact layer, both of which were n-type. The excess 10% Ga mole fraction, added into the barrier layer, has been reported to have the advantage of suppressing the oxidation of the exposed barrier surface when the Al fraction is high [17].

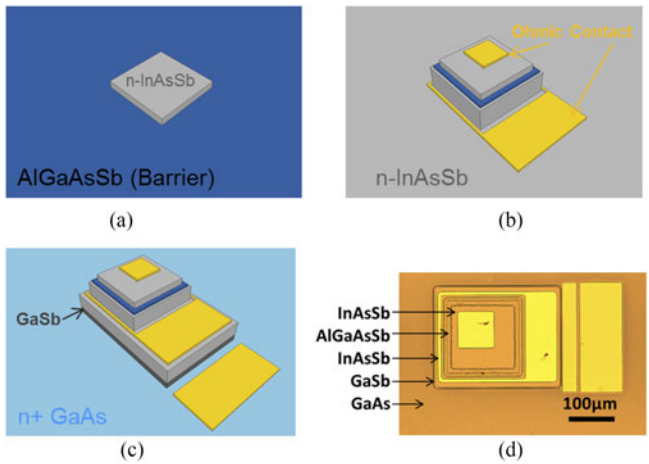

Fig. 3. Main process flow for fabrication of InAsSb/GaSb/GaAs nBnBn photodetector. (a) Etching of the top InAsSb contact layer. (b) Finish of the 1st mesa etching and formation of Ohmic contacts to the InAsSb contact layers. (c) Finish of the 2nd mesa etching and formation of Ohmic contact to the n+ GaAs contact layer. (d) Micrograph of a 150 μm × 150 μm complete device.

Fig. 3 shows the device fabrication flow that began with the mesa etching steps. First a positive photoresist mask (Shipley S1818) was patterned onto the sample followed by wet etching the top n-type InAsSb layer using a citric acid:H_2O_2:H_2O (2:1:6 by weight) etchant. The barrier layer, made of the quaternary material AlGaAsSb, reacts very slowly with the citric acid etchant. Therefore, the first mesa etching was stopped once the barrier layer was reached [see Fig. 3(a)]. Using the same mask, a 2.5% Tetramethylammonium hydroxide (TMAH) solution (Microposit MF-319) was then applied to etch the unmasked AlGaAsSb barrier layer thus exposing the bottom n-type InAsSb contact layer for further processes. After etching through the AlGaAsSb barrier, the citric acid based etchant could be used again. The first mesa etch was completed after approximately 1 μm of the bottom InAsSb material had been removed. Ohmic contacts to both InAsSb contact layers were then formed simultaneously by metallisation and lift-off as shown in Fig. 3(b).

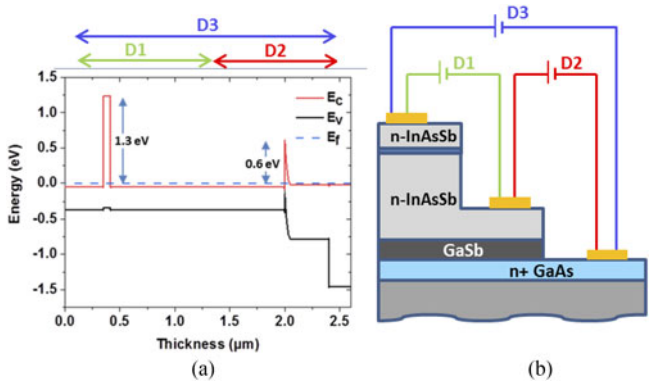

Fig. 4. (a) Band diagram of the proposed heterostructure at 300 K according to the model of Krijn [24]. (b) A sketch of the cross section of the fabricated nBnBn detector with three test-point pads to probe the nBn diode (D1), the InAsSb/GaSb/GaAs heterojunction diode (D2), and the combined nBnBn diode (D3) independently.

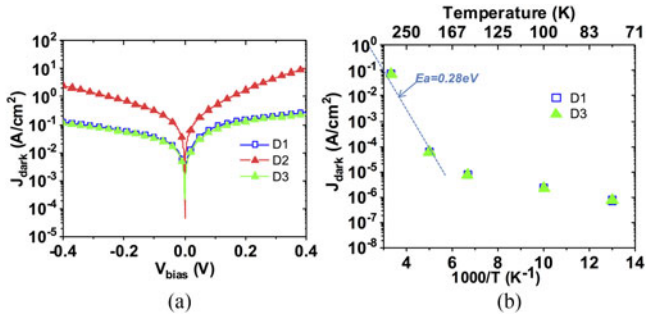

Fig. 5. (a) I-V characteristics for three junctions in the completed device. (b) Arrhenius plots of the dark current of D1 and D3, at −0.3 V applied bias.

The metal stack chosen for the nBn devices consisted of Ti 50 nm/Au 150 nm. Annealing of the contacts was not necessary as they showed Ohmic behavior at room temperature, owing to the narrow bandgap of InAsSb. The fabrication continued by etching a second mesa, also with the citric acid based etchant, to reach the GaSb buffer layer. Again the etch rate of GaSb for the etchant solution is negligible and the etch stops once the GaSb buffer layer is reached. Similarly, the MF-319 solvent was used to remove the GaSb buffer layer and expose the underlying n + GaAs contact layer. Finally, as shown in Fig. 3(c), a Pd/Ge/Au-based metal stack was evaporated on to the n + GaAs contact layer and annealed at 180 °C to induce Ohmic behaviour. The low temperature annealing avoids thermally-induced damage to the InAsSb material [22] and also has negligible effect on the previously formed Ohmic contacts. An optical micrograph of a completed nBnBn photodetector device with 150 μm × 150 μm active sensing area is shown in Fig. 3(d).

III. Results and Discussions

Fig. 4(a) shows the simulated band diagram of the photodetector device proposed in this work obtained with the software *Lumerical DEVICE*. It can be seen that the overall heterostructure of the device can be treated as a combination of a standard InAsSb nBn diode, an n-InAsSb/n-GaSb heterojunction diode, and an n-GaSb/IMF/n-GaAs heterojunction diode. The band position clearly indicates that there are two barriers in the conduction band: the AlGaAsSb barrier (∼1.3 eV) and the built-in potential (∼0.6 eV) created by the InAsSb/GaSb interface. The structure shown neglects the influence of interface states, created by the IMF growth of GaSb on GaAs, that have been shown to affect the actual bandstructure in similar previously reported structures, where a p-GaSb/IMF/n-GaAs heterojunction was formed [25]. Nevertheless, there is still lack of systematic study of the n-GaSb/IMF/n-GaAs interface. In this work, at the n-GaSb/n-GaAs interface it is assumed that these "acceptor-like" interface states have been compensated during the growth, hence have negligible effect on the overall bandstructure. For test purposes, each nBnBn device fabricated in this work has three test-point metal pads as shown in Fig. 4(b). Therefore, the standard nBn diode (D1), the InAsSb/GaSb/GaAs heterojunction diode (D2), and the combined nBnBn diode (D3) could be independently probed and their performance compared accordingly.

An Agilent 4155C semiconductor analyzer was used to characterize the current-voltage (I-V) curve of the fabricated devices. We made and characterized 70 identical devices. In each core the top mesa (D1) was 150 μm × 150 μm. The second mesa (D2) was 220 μm × 300 μm. Fig. 5(a) shows the measured typical I–V characteristics of D1, D2 and D3 at room temperature. Since D1 and D3 show approximately the same dark current level at all temperatures we measured, the current in D1 and D3 is thought to be confined in the top mesa area. Therefore, the dark current density of both D1 and D3 was calculated using a mesa size of 150 μm × 150 μm. The results show that, as compared to D1 and D3, D2 presents a particularly higher dark current (by approximately one order of magnitude) when a very small bias voltage is applied. D1 and D3 instead give very similar levels of dark current performance regardless of the bias voltage. This behavior can be explained by the previous bandstructure calculation, in which the potential barrier formed at InAsSb/GaSb junction is much smaller than that formed by the AlGaAsSb barrier layer. Moreover, the measured I-V characteristics show no obvious rectifying behavior (resistor-like) under various bias conditions. This indicates that D1, D2 and D3 can be treated as an n-type doped photoconductors when biased for detecting light.

Fig. 5(b) shows the Arrhenius plots of the dark current of D1 and D3 measured under cryogenic cooling conditions in the range from 77 K to 300 K. It is obvious that D1 and D3 continue to show similar levels of dark of current. This confirms that, under all applied cooling conditions, no excess dark current would be introduced by combining the standard nBn structure with the InAsSb/GaSb/GaAs heterojunction. The activation energy, extracted by fitting the measured results of D3, is 0.28 eV under −0.3 V bias. Despite the fact that the whole device was grown on a SI GaAs substrate, the value of activation energy is comparable to that obtained from nBn devices that were grown lattice-matched on to GaSb substrates [16], highlighting the good material quality obtained by the IMF growth. This result is also very close to the bandgap of the bulk InAsSb material (∼0.3 eV), indicating significant suppression of the dark current

TABLE I
COMPARISON OF MEASURED R0A VALUES AND DARK CURRENT UNDER ROOM TEMPERATURE

	GaSb doping (cm^{-3})	InAsSb doping (cm^{-3})	Substrate	$R \cdot A$ @300K (Ωcm^2) V_{bias}=0V (Low QE)	$R \cdot A$ @300K (Ωcm^2) V_{bias}= -0.3V (High QE)	J_{dark} @300K (Acm^{-2}) V_{bias}= -0.3V
Ref [18]	1×10^{18}	1×10^{16}	GaSb (n)	~3	0.01 to 0.1	~1
Ref [19]	5×10^{17}	5×10^{15}	GaSb (n)	0.6	…	5
Ref [20]	2×10^{17}	6×10^{16}	GaSb (n)	~0.5	…	~0.5
D2	5×10^{17}	5×10^{17}	GaAs (SI)	0.4	0.22	1.35
D3	5×10^{17}	5×10^{17}	GaAs (SI)	2.33	3.76	0.08

associated with the well-known Shockley–Read–Hall (SRH) process hence the capability of near room temperature operation. The slightly smaller value of activation energy as compared to the bandgap is thought to be due to the absence of passivation on the fabricated device. The hypothesis is supported by the fact that similar photodetectors that were previously reported did not suffer such degradation in active energy. In those reported devices, the mesa etching was stopped once arriving the barrier layer, whereas in this work the sidewall of all active layers had to be exposed in order to complete the devices. At temperatures below 160 K the activation energy decrease significantly to ~0.1 eV, indicating the SRH generation-recombination current and the surface leakage current start to dominate.

The "resistance.area" product (R·A) is a widely used figure of merit for comparing the performance of infrared photodetectors. When zero bias is applied, this product is called R_0A. Generally, if the detector is operating without bias, higher value of R_0A indicates smaller thermally-generated current noise and hence a better device. A comparison of typical R_0A and dark current values between this work and previously reported dual-color InAsSb/GaSb detectors is given in Table 1. Despite the difference in doping level and substrates used, all devices show comparable R_0A values at room temperature. However, a small reverse bias up to −0.3 V is normally applied to these devices in order to maximize their quantum efficiency (QE) and hence reach their best detection performance. Table 1 thus also shows the R·A values with −0.3 V reverse bias applied together with the corresponding level of dark current. Under reverse bias conditions, it is expected that the shot noise will begin to dominate. As the table shows, the R·A value of all InAsSb/GaSb heterojunction based devices, including D2, drops dramatically because of the excess leakage current under the $V_{bias} = -0.3$ V condition. The R·A value of the nBnBn diode (D3) is not as heavily affected when the negative bias is increased, since its dark current density (also shown in Table 1) is much smaller than that of the nBn devices.

The relative photo-response spectrum of the devices was measured with infrared light illumination, using a Bruker Vertex 70 FTIR spectrometer. Measurements were first carried out at room temperature and in standard atmosphere. Fig. 6(a) shows the spectra obtained from D2 for various values of V_{bias}. D2 shows a peak in photo-response at a wavelength of 1.6 μm, the magnitude of which increased by application of a negative bias. The cut-off wavelength of the photo-response for D2 is 2.1 μm, consistent with photon absorption in the GaSb buffer layer. No

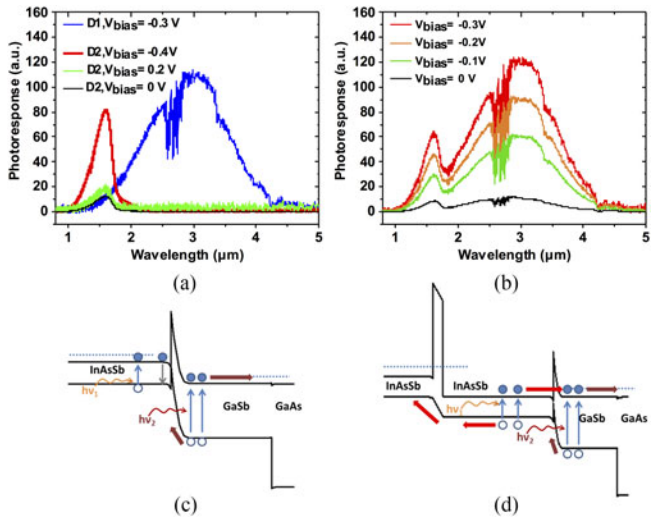

Fig. 6. Relative spectral response of D1, D2 (a) and D3 (b) under various bias conditions. (c) and (d) show the schematic of the proposed dual-color peak detection mechanism of the nBnBn structure.

photo-response from the InAsSb layer (expected in the 2 to 4 μm wavelength range) could be detected when a negative bias is applied to D2, and this is in good agreement with what reported by *Lackner et al.* [19]. The simulated band diagram in Fig. 6(c) shows the mechanisms underlying the operation of D2: photo-generated carriers in the InAsSb layer cannot be extracted due to the barrier at the InAsSb/GaSb interface, where they recombine. In contrast, the built-in potential allows extraction of the carriers generated in the GaSb layer. The principle of operation of D2 is therefore analogous to that of a metal semiconductor Schottky photodetector. On the other hand, both *Sharabani et al.* [18] and *Lackner et al.* [19] reported dual-color IR (SWIR and MWIR) detection capability for similar heterostructures to D2 (InAsSb/GaSb detectors) when a positive bias was applied. However, D2 shows no extension of cut-off wavelength for positive voltages up to 0.2 V, beyond which it was not possible to collect spectra due to the high level of dark current.

The photo-response of D1 and D3 was also measured. Under negative bias, D1 showed a photo-response spanning wavelengths from 1.5 μm to 4.6 μm with a peak response at 3 μm (see Fig. 6(a)). When compared to some state-of-the-art nBn photodetectors, the photoresponse of D1 in the MWIR is found to be smaller despite the similar composition of their absorption layers [11], [12]. The difference was attributed to the increase of bandgap (50–80 meV) due to the high doping level in the InAsSb absorption layer used [16]. The photo-response from D3 instead showed two clear and distinct peaks, at 1.6 μm and 3 μm [see Fig. 6(b)]. The dual peak indicates the extraction of carriers from both the GaSb and InAsSb absorption layers. The simulated band diagram in Fig. 6(d) shows that the nBnBn structure allows carriers generated in the thick InAsSb absorption layer to tunnel through the potential barrier created at the InAsSb/GaSb interface, hence to be extracted as photocurrent. When a positive voltage (not shown in Fig. 6) is applied, D3 and D1 show similar response spectra and only the InAsSb response is visible.

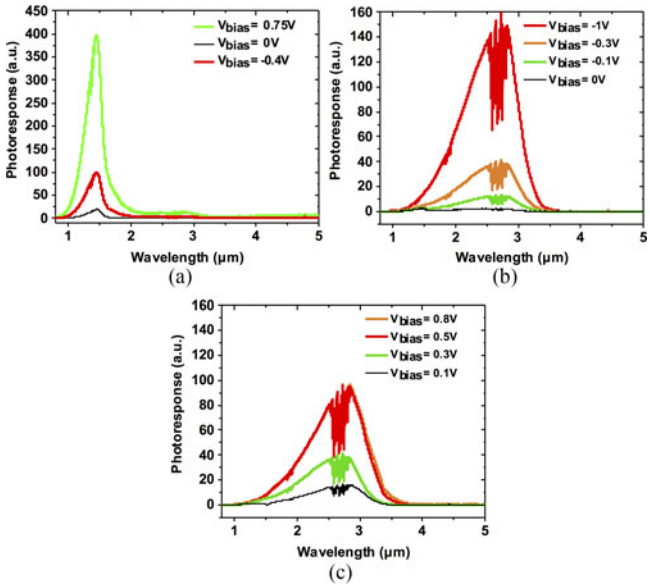

Fig. 7. Relative spectral response of D2 (a) and D3 (b) (c), under several bias conditions at 120 K.

Photo-response spectra were also measured with the devices kept at a temperature of approximately 120 K. At low temperature, by significantly eliminating the thermally generated carriers, larger bias voltages of up to 2 V could be applied without damage occurring to the device. The scan results obtained from D2 under cooling conditions are shown in Fig. 7(a). Similar to the results at room temperature, only the photo-response from the GaSb layer could be seen when a reverse bias was applied. However, different from the room temperature case, D2 presented the maximum photo-response when a positive bias $V_{bias} = 0.75$ V was applied. Moreover, as the inset of Fig. 7(a) shows, the cut-off wavelength of D2 was extended to the mid-IR wavelengths at this bias, despite being smaller than the SWIR response by approximately one order of magnitude. It is thought that the photo-response at mid-IR wavelengths is due to absorption in the InAsSb layer.

Fig. 7(b) and (c) show the photo-response spectra measured from D3 at 120 K. As compared to the results obtained at room temperature, the cut-off wavelength of D3 is shifted to 3.5 μm, consistent with an increase in the InAsSb bandgap. A larger bias voltage ($V_{bias} = -1$V) was required for the photo-generated carriers to tunnel through the InAsSb/GaSb potential barrier and thus maximize the photo-response. Even with large bias applied the dual-peak behavior of D3 becomes almost invisible, suggesting strong recombination of carriers generated in the GaSb layer under cryogenic cooling condition.

To measure the responsitivity of the complete nBnBn device, D3, was measured using a fiber-coupled 1.55 μm laser (SanTec TSL-550) at room temperature. A current responsivity R_i of approximately 0.15 A/W at $V_{bias} = -0.3$ V was extracted from the measurements. The corresponding value of quantum efficiency (QE) was found to be 12%, comparable to previously reported nBn detectors grown on GaAs substrate (QE = 22% in [17]) and GaSb substrate (QE $=\sim$ 8% in [16]). Considering both the shot noise and the thermal noise, the specific detectivity D$*$, given by the following expression

$$D^* = \frac{R_i}{\sqrt{2qJ_{dark} + 4kT/RA}}$$

was calculated to be 8.6×10^8 cm$\cdot$ Hz$^{1/2}$W^{-1}. According to the relative photoresponse results obtained with FTIR system, D$*$ at the peak wavelength (3μm) was estimated to be 1.7×10^9 cm $\cdot$ Hz$^{1/2}$W^{-1}. D$*$ is expected to increase by approximately two orders of magnitude (i.e., to 1×10^{10} Hz$^{1/2}$W^{-1}) at 200 K because of the measured reduction in dark current [see Fig. 5(b)].

IV. Summary

We have demonstrated a novel nBnBn heterostructure that supports dual-color infrared detection and growth on to a SI GaAs substrate. The complete device hybridizes a standard InAsSb-based nBn detector with an InAsSb/GaSb heterojunction detector. At high operating temperatures (>160 K), by blocking the majority current flow with a wide bandgap barrier layer, this nBnBn design does not suffer from the high leakage current (or high shot noise) that affected the previously investigated InAsSb/GaSb detectors when a bias was applied. The device that we present demonstrates a reduction in the dark current density of more than an order of magnitude at room temperature and more than three orders of magnitude at 200 K, in comparison with previous InAsSb/GaSb detectors. The specific detectivity of our completed device is also comparable to the best prior art for an InAsSb-based nBn detector. Additionally the device can detect both the SWIR and MWIR ranges at room temperature and hence further optimization of the device structure could lead to selectable dual-color operation. Future designs may focus on the demonstration of mid-IR avalanche photodiodes (APD), where the absorption and multiplication functions are assigned to the InAsSb and GaAs layers respectively [26]. All photodetector layers were grown monolithically on GaAs active layers hence this design has great potential to deliver cost-effective single-chip imaging arrays for civilian applications without the need for costly flip-chip bonding and cryogenic cooling.

Acknowledgment

The authors would like to thank all the staff of James Watt Nanofabrication Centre (JWNC) at University of Glasgow for their assistance. The authors would also like to thank Dr. Y. Fu at University of Glasgow for his help with low temperature measurements.

References

[1] P. Martyniuk, J. Antoszewski, M. Martyniuk, L. Faraone, and A. Rogalski, "New concepts in infrared photodetector designs," *Appl. Phys. Rev.*, vol. 1, no. 4, 2014, Art. no. 041102.
[2] A. Krier, *Mid-Infrared Semiconductor Optoelectronics*. London, U.K.: Springer, 2006.
[3] J. Sandsten, H. Edner, and S. Svanberg, "Gas visualization of industrial hydrocarbon emissions," *Opt. Exp.*, vol. 12, no. 7, pp. 1443–1451, 2004.
[4] J. Antoszewski, "Recent developments in mercury cadmium telluride IR detector technology," in *Proc. ECS Meet. Abstracts*, vol. 69, no. 14, pp. 61–75, 2015.

[5] D. Lee *et al.*, "High-operating temperature HgCdTe: A vision for the near future," *J. Electron. Mater.*, vol. 45, pp. 4587–4595, 2016.

[6] N. D. Akhavan, G. Jolley, G. A. Umana-Membreno, J. Antoszewski, and L. Faraone, "Performance modeling of bandgap engineered HgCdTe-Based nBn infrared detectors," *IEEE Trans. Electron Devices*, vol. 61, no. 11, pp. 3691–3698, Nov. 2014.

[7] A. Soibel *et al.*, "Room temperature performance of mid-wavelength infrared InAsSb nBn detectors," *Appl. Phys. Lett.*, vol. 105, no. 2, 2014, Art. no. 023512.

[8] "European commission - PRESS RELEASES - Press release - EU protects citizens from toxic mercury, paves the way for global action," Europa.eu, 2018. [Online]. Available:http://europa.eu/rapid/press-release_IP-17-1345_en.htm

[9] C. Downs and T. Vandervelde, "Progress in infrared photodetectors since 2000," *Sensors*, vol. 13, no. 4, pp. 5054–5098, 2013.

[10] S. Maimon and G. Wicks, "nBn detector, an infrared detector with reduced dark current and higher operating temperature," *Appl. Phys. Lett.*, vol. 89, 2006, Art. no. 15110913.

[11] A. Soibel *et al.*, "Room temperature performance of mid-wavelength infrared InAsSb nBn detectors," *Appl. Phys. Lett.*, vol. 105, no. 2, 2014, Art. no. 023512.

[12] S. Myers *et al.*, "Performance of InAsSb-based infrared detectors with nBn design," in *Proc. SPIE Int. Soc. Opt. Eng.*, 2010, 3 pages, Art. no. 7808.

[13] S. Huang, G. Balakrishnan, and D. Huffaker, "Interfacial misfit array formation for GaSb growth on GaAs," *J. Appl. Phys.*, vol. 105, no. 10, 2009, Art. no. 103104.

[14] D. Benyahia *et al.*, "Interfacial misfit array technique for GaSb growth on GaAs (001) substrate by molecular beam epitaxy," *J. Electron. Mater.*, vol. 47, no. 1, pp. 299–304, 2017.

[15] W. Sarney, S. Svensson, Y. Xu, D. Donetsky, and G. Belenky, "Bulk InAsSb with 0.1 eV bandgap on GaAs," *J. Appl. Phys.*, vol. 122, no. 2, 2017, Art. no. 025705.

[16] A. Craig *et al.*, "InAsSb-based nBn photodetectors: Lattice mismatched growth on GaAs and low-frequency noise performance," *Semicond. Sci. Technol.*, vol. 30, no. 10, 2015, Art. no. 105011.

[17] A. Craig, A. Marshall, Z. Tian, S. Krishna, and A. Krier, "Mid-infrared $InAs_{0.79}$ $Sb_{0.21}$-based nBn photodetectors with $Al_{0.9}Ga_{0.2}As_{0.1}Sb_{0.9}$ barrier layers, and comparisons with $InAs_{0.87}Sb_{0.13}$ p-i-n diodes, both grown on GaAs using interfacial misfit arrays," *Appl. Phys. Lett.*, vol. 103, no. 25, 2013, Art. no. 253502.

[18] Y. Sharabani, Y. Paltiel, A. Sher, A. Raizman, and A. Zussman, "InAsSb/GaSb heterostructure based mid-wavelength-infrared detector for high temperature operation," *Appl. Phys. Lett.*, vol. 90, no. 23, 2007, Art. no. 232106.

[19] D. Lackner *et al.*, "Electrical and optical characterization of n-InAsSb/n-GaSb heterojunctions," *J. Appl. Phys.*, vol. 107, no. 1, 2010, Art. no. 014512.

[20] J. Tong *et al.*, "Study of dual color infrared photodetection from n-GaSb/n-InAsSb heterostructures," *AIP Adv.*, vol. 6, no. 2, 2016, Art. no. 025120.

[21] V. Pusino *et al.*, "InSb photodiodes for monolithic active focal plane arrays on GaAs substrates," *IEEE Trans. Electron Devices*, vol. 63, no. 8, pp. 3135–3142, Aug. 2016.

[22] C. Xie *et al.*, "Monolithic integration of an active InSb-Based mid-infrared photo-pixel with a GaAs MESFET," *IEEE Trans. Electron Devices*, vol. 62, no. 12, pp. 4069–4075, Dec. 2015.

[23] C. Xie *et al.*, "Single-chip, midinfrared array for room temperature video rate imaging," *Optica*, vol. 4, no. 12, pp. 1498–1502, 2017.

[24] M. Krijn, "Heterojunction band offsets and effective masses in III–V quaternary alloys," *Semicond. Sci. Technol.*, vol. 6, no. 1, pp. 27–31, 1991.

[25] M. Aziz *et al.*, "Electrical behavior of MBE grown interfacial misfit GaSb/GaAs heterostructures with and without te-doped interfaces," *IEEE Trans. Electron Devices*, vol. 62, no. 12, pp. 3980–3986, Dec. 2015.

[26] A. Marshall, A. Craig, C. Reyner, and D. Huffaker, "GaAs and AlGaAs APDs with GaSb absorption regions in a separate absorption and multiplication structure using a heterolattice interface," *Infrared Phys. Technol.*, vol. 70, pp. 168–170, 2015.

Chengzhi Xie received the B.Eng. degree from the College of Precision Instrument and Optoelectronics Engineering, Tianjin University, Tianjin, China, in 2012, and the Ph.D. degree from the School of Engineering, University of Glasgow, Glasgow, U.K., in 2017. He is currently a Research Assistant with the University of Glasgow focusing on the implementation of the monolithically integrated mid-IR imaging array devices.

Vincenzo Pusino received the M.Sc. degree in electronics and electrical engineering from the University of Pavia, Pavia, Italy, in 2008, and the Ph.D. degree from the School of Engineering, University of Glasgow, Glasgow, U.K., in 2014. He is currently a Research Associate with the University of Glasgow. His current research interests include mid-IR imaging, III–V semiconductors, semiconductor lasers, integrated nonlinear optics, and photonics.

Ata Khalid received the Ph.D. degree from King's College London, London, England, in electronic device engineering in 2000. He worked several years in King's College London to develop MMIC design and fabrication, development of HBTs and HEMTs. In 2004, he moved to the school of engineering at University of Glasgow to develop solid state THz radiation source technology based on planar Gunn diodes. In September 2017, he joined Cranfield University, Cranfield, England, as Lecturer in Sensors and Sensor Systems. He is member of Institute of Physics (IOP).

Adam P. Craig received the MPhys degree in physics in 2011 from Lancaster University, Lancashire, England, where he is currently working toward the Ph.D. degree. After graduating in 2011, he was appointed as an R.A. working in the group of A. R. J. Marshall. His current interests include the development of resonant cavity infrared detectors and eSWIR single photon avalance photodiodes.

Andrew Marshall is currently a Lecturer in Physics Department, Lancaster University, Lancashire, England, with more than 10 years of experience researching novel infrared detector, emitters and the fundamentals of III-V materials. After graduating, he initially worked in the automotive industry for 5 years before returning to Sheffield University to study for an industry sponsored Ph.D. degree and work as a Researcher. In 2010, he won a prestigious Royal Academy of Engineering research fellow and moved to Lancaster University.

David R. S. Cumming received the B.Eng. degree from University of Glasgow, Glasgow, Scotland, and the Ph.D. degree from University of Cambridge, Cambridge, England. He holds the Chair of Electronic Systems with the University of Glasgow, Glasgow, Scotland. He is currently a Director of the Electronics Design Centre for Heterogeneous Systems and leads the Microsystem Technology Group in the School of Engineering. He works on sensor systems and technologies for biomedical and imaging applications. He is a Founder of Mode Diagnostics and worked with Ion Torrent that commercialized his CMOS sensor technology for use in gene sequencing. He is FRSE, FIEEE, and FIET, and holds a Royal Society Wolfson Merit Award.